

Rapid afterslip following the 1999 Chi-Chi, Taiwan Earthquake

Ya-Ju Hsu,^{1,2} Noa Bechor,³ Paul Segall,³ Shui-Beih Yu,¹ Long-Chen Kuo,¹ and Kuo-Fong Ma²

Received 21 February 2002; revised 11 April 2002; accepted 16 May 2002; published 16 August 2002.

[1] Postseismic displacements of as much as 14 cm were recorded by GPS measurements in the 3 months following the M_w 7.6 1999 Chi-Chi, Taiwan earthquake. Data from 35 continuous and 90 campaign-surveyed stations, which show continued east over west thrusting, are analyzed to estimate the postseismic slip distribution and fault geometry. Assuming the shallow fault dips 24° E, as determined by numerous studies of the mainshock, we invert for the deeper fault structure. Our results show that the fault dip shallows with depth below the hypocenter, merging into a nearly horizontal decollement at a depth of 8–12 km. The afterslip distribution shows a maximum slip of 25 cm in the hypocentral region at 7–12 km depth as well as significant slip on the lower decollement. Afterslip is notably absent in the region of maximum coseismic slip, consistent with the afterslip being driven by the mainshock stress change. **INDEX TERMS:** 1242 Geodesy and Gravity: Seismic deformations (7205); 1243 Geodesy and Gravity: Space geodetic surveys; 3210 Mathematical Geophysics: Modeling

1. Introduction

[2] The 21 September 1999 Chi-Chi Taiwan earthquake ($M_w = 7.6$) resulted from the reactivation of the Chelungpu fault, a major frontal thrust within the Taiwan collision belt. It broke the ground surface causing a 100-km-long surface rupture that trends north-south, except for an east-west trending segment at the northern end of the rupture near Fengyuan [Lee *et al.*, 2002]. The GPS observations show NW-NNW directed horizontal movements of 1.1–9.1 m and vertical uplift of 1.2–4.4 m on the hanging wall. In contrast, much smaller SE-SEE directed horizontal movements of 0.1–1.5 m and slight subsidence of 0.02–0.26 m are found on the footwall [Yu *et al.*, 2001].

[3] The observed GPS coseismic displacements, as well as seismic waveforms, were used in combined inversions by various authors to constrain the ruptured fault geometry [e.g. Dominguez *et al.*, 2001; Ji *et al.*, 2001; Loevenbruck *et al.*, 2001; Ma *et al.*, 2001; Zeng and Chen, 2001]. All of these studies find a main north-south striking fault, dipping 20° – 30° to the east. The fault slip increases from less than 3 m on the southern part of the fault to a maximum of about 10 m on the northern end where the fault curves to east. Most of the slip is shallower than the hypocentral depth of 8 km [e.g. Johnson *et al.*, 2001].

[4] Displacements of as much as 14 cm were measured by GPS in the first three months following the earthquake [Yu *et al.*, 2001]. Preliminary analysis suggests these data are well explained by afterslip, rather than either viscoelastic or poroelastic relaxation [Bechor *et al.*, 2001]. Here we analyze the postseismic displacements

to determine the distribution of afterslip and the deep fault geometry. Most aftershocks occurred below the mainshock, however the aftershock distribution alone does not clearly resolve the fault structure [Chang *et al.*, 2000; Cheng, 2000; Chen *et al.*, 2002; Hirata *et al.*, 2000].

2. Data Collection and Processing

[5] After the Chi-Chi earthquake, seven continuously recording GPS stations were installed in the epicentral region, in addition to 3 pre-existing continuous stations. About 80 campaign-surveyed stations in central Taiwan were surveyed up to 7 times from September 1999 to December 2000 through a joint effort by Academia Sinica and the Land Survey Bureau, Ministry of Interior. These stations are spaced roughly 5–10 km along and across the fault zone. The GPS data are processed with Bernese 4.2 software using a fiducial free approach. Precise ephemerides provided by the International GPS Services (IGS) are employed and fixed in the post-processing. Residual tropospheric zenith delays are estimated simultaneously with the station coordinates by least-squares adjustment. Yu *et al.* [2001] provided a more detailed description of the data acquisition and processing.

[6] Horizontal postseismic displacements on the footwall of the Chelungpu fault are mostly less than 2 cm in the 3 months after the Chi-Chi earthquake. Footwall vertical displacements are unsystematic, with the majority less than 2 cm. In contrast, west or west-northwest directed horizontal displacements of up to 14 cm are observed on the hanging wall of the Chelungpu fault in the same time period (Figure 1). Significant uplift of up to 10 cm is also found here. Because the fault trace is geometrically complex, we remove a few stations very close to the surface rupture to avoid having stations located on the wrong side of the planar model-fault. We include numerous additional continuous and campaign-surveyed stations distributed around the island of Taiwan.

[7] To remove the effect of secular deformation we use the preseismic GPS velocity field estimated by Yu *et al.* [2001]. Velocities for sites which were not analyzed by Yu *et al.* [2001] are determined by interpolation of the existing data. The secular displacements are removed from each postseismic epoch prior to further analysis, and errors in the secular correction are propagated in to the data. The maximum secular correction is approximately 1 cm.

[8] In order to compute the postseismic displacement for a specified time interval, we must account for the fact that campaign-surveyed stations were observed at different times. To do so we assume an exponential decay of the form $a_0 + a_1 \exp(-t/\tau)$ where t is time since the mainshock. We determine the exponential decay constant τ by dividing Taiwan into four regions: footwall, northern and southern sections of the hanging wall within 20 km of the surface rupture, and the remaining far field. Each region is assigned an exponential decay constant from a representative continuous station (Stations KZON, S016, I007, and 5936 are chosen to represent the four regions with relaxation times of 206, 330, 159, and 233 days, respectively). We then solve for the best fitting coefficients a_0 and a_1 , accounting for the correlations between stations, and estimate the cumulative displacement for the 3 months period from 0 to 97 days after the earthquake (Figure 2). Interpolation errors are propagated formally into the displacements. Due to

¹Institute of Earth Sciences, Academia Sinica, Nankang, Taipei, Taiwan, R.O.C.

²Institute of Geophysics, National Central University, Chungli, Taiwan, R.O.C.

³Geophysics Department, Stanford University, California, USA.

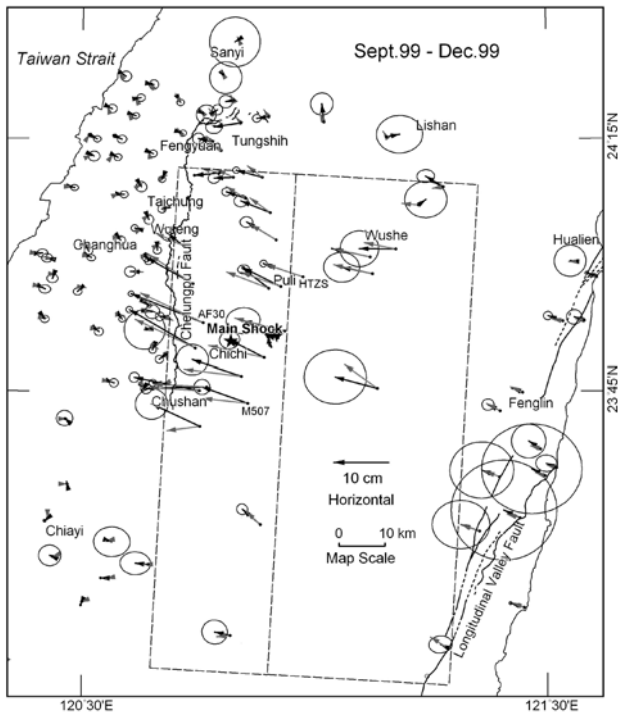


Figure 1. Observed (dark vectors with 95% confidence ellipses) and predicted (light vectors) horizontal postseismic displacements from 0 to 97 days after the Chi-Chi earthquake. The predicted displacements are computed for the best fitting slip distribution and fault geometry (see text). Heavy curved line denotes the surface rupture. The surface projection of the model fault planes are shown as rectangles. The star indicates the mainshock epicenter.

the low signal to noise ratio in the vertical components of the campaign data we choose to model only the horizontal components.

[9] The postseismic displacement field is summarized in Figure 1. West-northwest directed displacements of the hanging-wall sites are prominent. Displacements are greater in the southern part of the rupture near Chi-Chi than to the north where the maximum coseismic displacements occurred. Note also that there are significant postseismic displacements on the east coast of Taiwan, 100 km east of the fault rupture, as well as 50 km south of the southern end of the fault break. This indicates deformation at depths significantly greater than in the mainshock.

3. Method

[10] In order to invert for the afterslip distribution as well as fault geometry we minimize the following functional:

$$F(\mathbf{s}, \beta, \mathbf{m}) = \left\| \sum^{-1/2} (G(\mathbf{m})\mathbf{s} - \mathbf{d}) \right\|^2 + \beta^2 \|\nabla^2 \mathbf{s}\|^2$$

where $\Sigma^{-1/2}$ is the inverse square root of the data covariance matrix, $G(\mathbf{m})$ is a matrix of elastic half-space Green's functions for rectangular faults [e.g., Okada, 1985], which depend on the fault geometry parameters \mathbf{m} (i.e. fault dip, depth, etc), \mathbf{s} is slip, \mathbf{d} is the observed displacements and the smoothing operator ∇^2 is the finite difference approximation of the Laplacian operator. β serves as the weighting of the model roughness versus data misfit, and is obtained by cross-validation [Matthews and Segall, 1993].

[11] The shallow fault geometry, which was well resolved by the coseismic displacements [Johnson et al, 2001], is fixed to a NS striking plane dipping 24° E to a depth of roughly 8 km. Below this it has been suggested that the Chelungpu fault merges with a shallowly dipping decollement based on balanced geological cross-

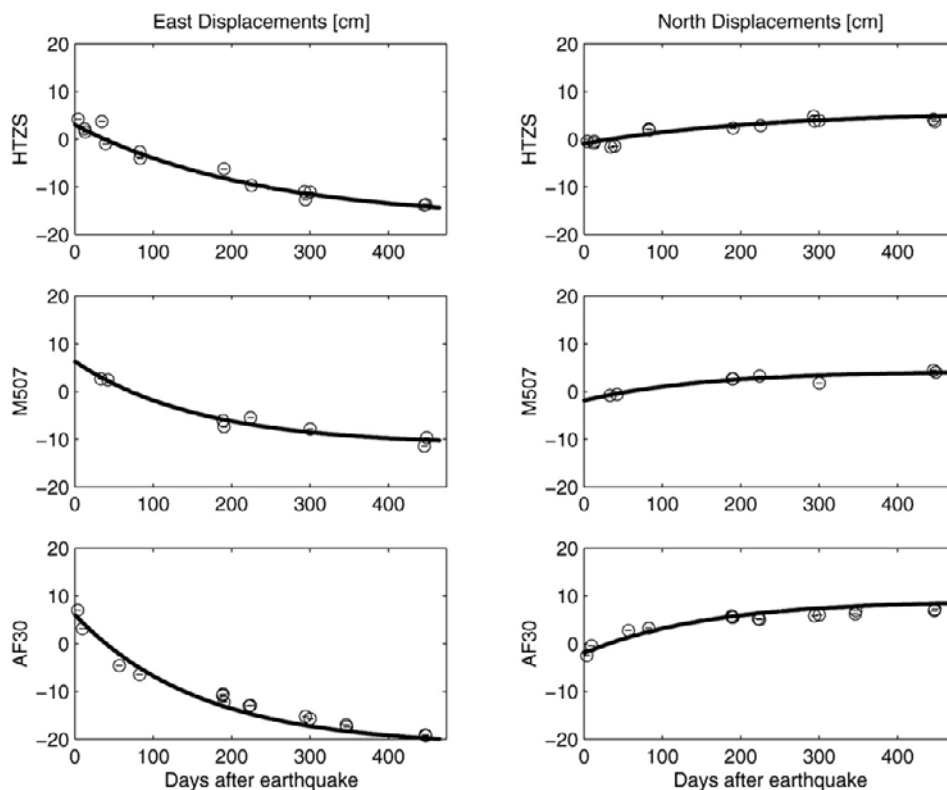


Figure 2. Time series of displacements following the Chi-Chi earthquake for typical hanging wall sites. Fits to an exponential decay are indicated.

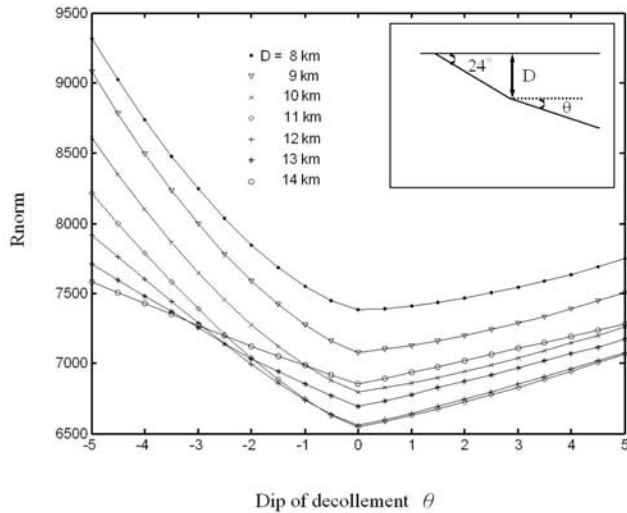


Figure 3. Data misfit as a function of dip of the lower fault segment (θ) for different hinge depths (D). Model geometry is shown in the inset.

sections [Suppe and Jamson, 1979]. Loevenbruck *et al.* [2001] fitted the interseismic velocities measured from Taiwan GPS network between 1990 and 1995 using this fault geometry with a 10 km deep decollement. Dominguez *et al.* [2001] used a similar fault geometry with a 6–10° dipping decollement at a depth of 7–8 km to model the coseismic displacement. Their results showed little coseismic slip on the decollement.

[12] We model a two-segment fault with dip θ below a hinge at depth D (Figure 3). Following Johnson *et al.* [2001] we search a range of θ and D , estimating the optimal slip distribution for each fault geometry. We vary the hinge depth D from 4 km to 20 km, and the dip of the deeper segment θ from -5° to 20° . The width of the deeper segment is kept constant at 40 km. β is fixed at the cross validation result for $D = 10$ km, and $\theta = 0^\circ$. In all the models we keep the number of fault patches constant. Because significant postseismic displacement was observed well south of the fault rupture (Figure 1 and Yu *et al.* [2001]), we allow the model fault to extend 110 km along strike (Figure 1).

4. Results and Discussions

[13] A preliminary analysis suggests a minimum in the weighted residual norm with D between 8 and 14 km and θ between -5° and 5° . We then refine the grid about the minimum to obtain the optimal fault parameters as shown in Figure 3. The conclusion is that the data are best fit by a nearly horizontal decollement at a depth of between 11 and 12 km. We also test the effect of including the EW trending structure at the northern end of the surface rupture, slip on which was required to fit the coseismic displacements [Johnson *et al.*, 2001]. We find that including the EW fault in the postseismic model does not significantly change the fit to the postseismic data. With this fault included the optimal hinge depth is slightly shallower (~ 8 km) but the deeper segment is still subhorizontal. The optimal model explains 93% of the variance in the GPS data.

[14] Hirata *et al.* [2000] found a 30° east-dipping plane and a nearly horizontal plane at a depth of ~ 10 km, which may correspond to the decollement, based on the location of 736 aftershocks. Chen *et al.*'s [2002] aftershock relocations also suggest a nearly horizontal decollement at a depth of 8 to 12 km. The similarity between the GPS and aftershock derived fault geometries adds strength to the thin-skinned model of active tectonics in Taiwan. Seismic reflection profiles [Wang, 2001] also

suggested the existence of a horizontal decollement beneath the Chelungpu fault.

[15] The afterslip distribution corresponding to the best fitting fault geometry (Figure 4a) shows that afterslip is concentrated south and down-dip of the largest coseismic slip (Figure 4b). The maximum postseismic slip of 25 cm occurs in the hypocentral region at 7–12 km depth. Significant slip, about half of maximum, occurs on the lower decollement. In contrast, there is little or no slip in the area of maximum coseismic slip, consistent with the idea that afterslip is driven by the stress change due to the mainshock. We also find slip on the southern end of the decollement (Figure 4a) as noted by Yu *et al.* [2001]. The inferred afterslip moment is approximately 2.1×10^{19} N-m, or about 7% of the mainshock moment. The total moment released by aftershocks is 1.6×10^{19} N-m during the same interval and area [Hohn Kao, personal communication], indicating that a significant amount of the postseismic deformation is aseismic.

5. Conclusion

[16] Displacements of as much as 14 cm were observed by GPS in the first three months after the Chi-Chi earthquake. Constraining the shallow fault geometry, based on the surface rupture and

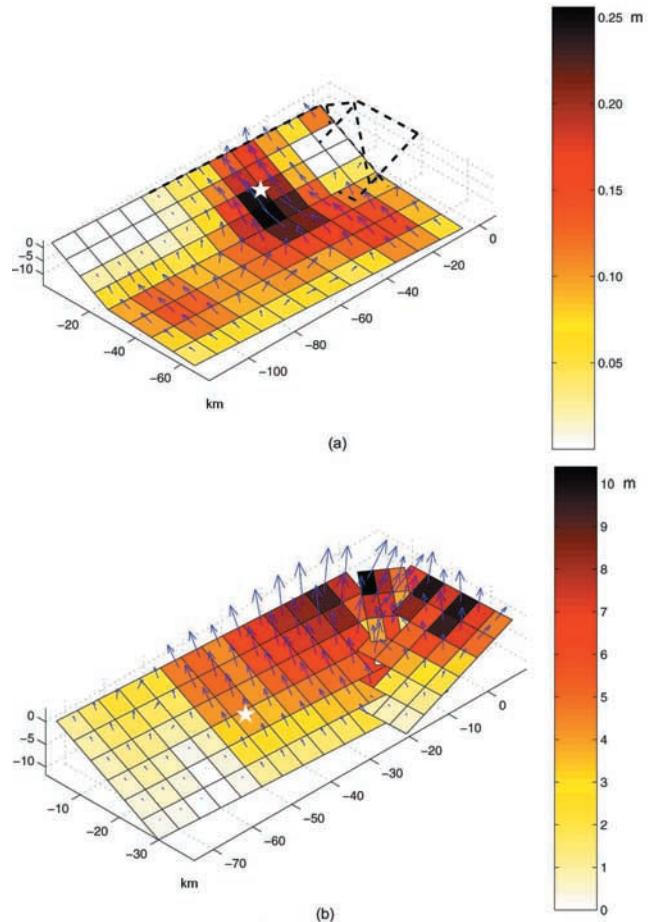


Figure 4. Comparison of postseismic and coseismic slip distributions. (a) The postseismic fault geometry and slip distribution. Slip on a shallow 24° dipping fault combined with a horizontal decollement at 11–12 km depth. The black dashed outline indicates additional segments needed to model the coseismic displacements. Star indicates mainshock hypocenter. (b) The coseismic fault geometry and slip distribution from Johnson *et al.* [2001].

coseismic displacements, to strike NS and dip 24° E, the data require a deeper horizontal decollement in the depth range of 8–12 km. The afterslip distribution shows maximum slip of 25 cm in hypocentral region and significant slip on the lower decollement and southern extension of the Chelungpu fault. In contrast, there is little if any afterslip in the area of maximum coseismic slip. This is expected given that stress transfer during the mainshock caused the afterslip. This study confirms the existence of a near horizontal decollement, and suggests that deep slip extended well south of the mainshock rupture.

[17] **Acknowledgments.** We are grateful to many colleagues at the Institute of Earth Sciences, Academia Sinica and the Land Survey Bureau, Ministry of Interior who have participated in collecting GPS data. We thank Kaj Johnson and Peter Cervelli for valuable suggestions. This study was supported by Academic Sinica and National Science Council of the Republic of China under Grant NSC 90-M-001-014 and the National Science Foundation. This is a contribution of the Institute of Earth Sciences, Academia Sinica, IESAS796.

References

- Bechor, N., P. Segall, Y. J. Hsu, and S. B. Yu, Time-dependent inversion for post-seismic slip following the 1999 Chi-Chi Taiwan earthquake using GPS observations, *EOS Trans., AGU*, 82(47), Nov. 2001.
- Chang, C. H., Y. M. Wu, T. C. Shin, and C. Y. Wang, Relocation of the 1999 Chi-Chi earthquake in Taiwan, *TAO*, 11, 581–590, 2000.
- Chen, K. C., B. S. Huang, J. H. Wang, and H. Y. Yen, Conjugate thrust faulting associated with the 1999 Chi-Chi Taiwan, earthquake sequence, *Geophys. Res. Lett.*, in press, 2002.
- Cheng, W. B., Three-dimensional crustal structure around the source area of the 1999 Chi-Chi earthquake in Taiwan and its relation to the aftershock locations, *TAO*, 11, 643–660, 2000.
- Dominguez, S., J. P. Avouac, and R. Michel, Horizontal coseismic deformation of the 2001 Chi-Chi earthquake measured from SPOT satellite images: Implications for the seismic cycle along the western foothills of Central Taiwan, *J. Geophysics Res.*, in press, 2001.
- Hirata, N., S. Sakai, Z. S. Liaw, Y. B. Tsai, and S. B. Yu, Aftershock observations of the 1999 Chi-Chi, Taiwan earthquake, *Bull. Earthquake Res. Inst., Tokyo Univ.*, 75, 33–46, 2000.
- Ji, C., D. V. Helmberger, T. R. A. Song, K. F. Ma, and D. J. Wald, Slip distribution and tectonic implication of the 1999 Chi-Chi, Taiwan, earthquake, *Geophys. Res. Lett.*, 28, 4379–4382, 2001.
- Johnson, K. M., Y. J. Hsu, P. Segall, and S. B. Yu, Fault geometry and slip distribution of the 1999 Chi-Chi, Taiwan earthquake imaged from inversion of GPS data, *Geophys. Res. Lett.*, 28, 2285–2288, 2001.
- Lee, J. C., H. T. Chu, J. Angelier, Y. C. Chan, J. C. Hu, C. Y. Lu, and R. J. Rau, Structural characteristics of northern surface ruptures of the 1999 $M_w = 7.6$ Chi-Chi, Taiwan earthquake, *J. Struct. Geol.*, 24, 173–192, 2002.
- Loevenbruck, A., R. Cattin, X. Pichon Le, M. L. Courty, and S. B. Yu, Seismic cycle in Taiwan derived from GPS measurements, *C.R. Acad. Sci. II*, 333, 57–64, 2001.
- Ma, K. F., J. Mori, S. J. Lee, and S. B. Yu, Spatial and temporal slip distribution of the Chi-Chi, Taiwan, earthquake from strong motion, teleseismic and GPS data, *Bull. Seism. Soc. Am.*, 91, 1069–1087, 2001.
- Matthews, M., and P. Segall, Statistical inversion of crustal deformation data and estimation of the depth distribution of slip in the 1906 earthquake, *J. Geophysics Res.*, 98, 12,153–12,163, 1993.
- Okada, Y., Surface deformation due to shear and tensile faults in a half-space, *Bull. Seism. Soc. Am.*, 75, 1135–1154, 1985.
- Suppe, J., and J. Jamson, Fault-bend origin of frontal folds of the western Taiwan fold-and-thrust belt, *Petro. Geol. Taiwan*, 16, 1–18, 1979.
- Wang, C. Y., Mapping the Chelungpu fault by seismic reflection methods, Proceed. of ICDP Workshop on Drilling the Chelungpu Fault, Taiwan, September 27–28, Taipei, Taiwan, 2001.
- Yu, S. B., L. C. Kuo, Y. J. Hsu, H. H. Su, C. C. Liu, C. S. Hou, J. F. Lee, T. C. Lai, C. C. Liu, C. L. Liu, T. F. Tseng, C. S. Tsai, and T. C. Shin, Preseismic deformation and coseismic displacements associated with the 1999 Chi-Chi, Taiwan, earthquake, *Bull. Seism. Soc. Am.*, 91, 995–1012, 2001.
- Zeng, Y., and C. H. Chen, Fault rupture process of the 20 September 1999 Chi-Chi, Taiwan, earthquake, *Bull. Seism. Soc. Am.*, 91, 1088–1098, 2001.

Y.-J. Hsu, S.-B. Yu, and L.-C. Kuo, Institute of Earth Sciences, Academia Sinica, P.O. Box 1-55, Nankang, Taipei, Taiwan, R.O.C. (yaru@earth.sinica.edu.tw)

K.-F. Ma, Institute of Geophysics, National Central University, Chungli, Taiwan, R.O.C.

N. Bechor and P. Segall, Geophysics Department, Stanford University, California, USA.